

# Interannual Changes in Stratospheric Constituents and Global Circulation Derived From Satellite Data

William J. Randel and Fei Wu

*Atmospheric Chemistry Division, National Center for Atmospheric Research, Boulder, CO*

J. M. Russell III

*Atmospheric Sciences, Hampton University, Hampton, VA*

J. M. Zawodny

*Atmospheric Chemistry Division, NASA Langley Research Center, Hampton, VA*

John Nash

*UK Meteorological Office, Bracknell, Berkshire, UK*

The characteristics of low-frequency interannual changes in stratospheric constituents are examined using measurements from the HALOE [1991-1999] and SAGE II [1984-1998] satellite instruments. Both the increasing H<sub>2</sub>O and decreasing CH<sub>4</sub> observations from the first several years of HALOE measurements are found to be absent (or partially reversed) in the data since ~ 1996. Ozone and NO<sub>x</sub> (NO + NO<sub>2</sub>) observations from HALOE also show 'trends' over ~ 1991-1995 that become flat in the latter record. Comparisons with the longer-term SAGE II measurements of ozone and NO<sub>2</sub> demonstrate that changes over the short period 1991-1995 are not representative of decadal-scale trends, but rather are episodic in nature. One possibility is that these changes reflect a prolonged response to the Mt. Pinatubo volcanic eruption in 1991. Stratospheric temperatures and derived circulation statistics are examined for the period 1979-1999. While Pinatubo produced enhanced tropical upwelling in the stratosphere for 1-2 years, other sources of stratospheric variability probably also contribute to low-frequency constituent 'trends.'

## 1. INTRODUCTION

Decadal-scale changes in temperature and circulation of the stratosphere and mesosphere are anticipated due to increases in greenhouse gas concentrations, and decreases in stratospheric ozone [e.g., WMO, 1999]. Similarly,

concentrations of constituents in the middle atmosphere are expected to change due to trends in tropospheric source gases (e.g., CO<sub>2</sub>, N<sub>2</sub>O, and CH<sub>4</sub>), trends in chlorine affecting ozone chemistry, and changes in dynamics and transport. Indeed, observed variations in long-lived constituents can be a sensitive measure of changes in (integrated) large-scale transport, which may not otherwise be observed in dynamical quantities directly. In addition to externally forced changes, the middle atmosphere can exhibit significant interannual variability due solely to internal dynamics [e.g., Scott and Haynes, 1998; Hamilton,

this volume]. Although constituent observations alone cannot identify 'forced' versus 'natural' changes, it is instructive to quantify the interannual variability in the long time series of data now available from satellites.

The long-term record (1991-present) of constituent observations from the Halogen Occultation Experiment (HALOE) [Russell *et al.*, 1993] has provided an unprecedented view of interannual variations in stratospheric constituents. Some of the most intriguing and unanticipated results from the first several years of HALOE data were observations of increasing water vapor throughout the stratosphere, together with decreasing CH<sub>4</sub> above 35 km [Nedoluha *et al.*, 1998a, b; Evans *et al.*, 1998; Randel *et al.*, 1999]. The causes of these trends are still unknown, and one key question is do these 'trends' continue in the longer record of HALOE measurements. HALOE has also observed trend-like changes in other constituents. Russell *et al.* [1996] used HALOE observations of increasing HF and HCl near the stratopause to show consistency with tropospheric emission rates, and effectively close the stratospheric budgets of chlorine and fluorine. The HF observations were updated by Considine *et al.* [1997] to show a slowdown in the rate of increase. Anderson *et al.* [2000] analyzed the HCl and HF time series through 1999, and tied the stratospheric changes to tropospheric source variations linked to the Montreal Protocol. Siskind *et al.* [1998] have studied the relationships between chlorine, methane and ozone changes observed by HALOE during 1992-1995, and Froidevaux *et al.* [2000] has quantified long-term changes in stratospheric chlorine compounds during the HALOE observing period.

The objective here is to update the HALOE constituent observations through 1999 to quantify the spatial and temporal characteristics of observed interannual changes. The H<sub>2</sub>O and CH<sub>4</sub> variations are shown to be coherent throughout the stratosphere and lower mesosphere, demonstrating interannual coupling between these regions. In order to provide a longer-term perspective on interannual variability, we include SAGE II observations of ozone and NO<sub>2</sub> for the period 1984-1998. These are the longest record of stratospheric constituents measured by a single satellite instrument, and it is instructive to compare the SAGE II and HALOE records of these same species. Finally, we briefly examine some diagnostics of changes in stratospheric circulation over the period 1979-1999. Although extensive diagnostics of constituent transport circulations are beyond the scope of this paper, we present some diagnostics of interannual changes in stratospheric temperature and planetary wave variability which give qualitative measures of large-scale circulation changes.

## 2. DATA AND ANALYSES

### 2.1. HALOE

The HALOE instrument uses solar occultation measurements to provide high quality observations of stratospheric H<sub>2</sub>O, CH<sub>4</sub>, HF, HCl, ozone, NO, and NO<sub>2</sub> [Russell *et al.*, 1993]. The HALOE data here are from the version 19 (v19) retrieval algorithm, spanning the time period October 1991 – December 1999. We use HALOE level 3a data, with vertical sampling on standard UARS pressure levels (6 per decade of pressure; vertical resolution of ~ 2.5 km). The H<sub>2</sub>O and CH<sub>4</sub> measurements extend over ~ 15-80 km, while the other species are analyzed here for ~ 15-55 km. Sunrise and sunset HALOE measurements are combined for all constituents except NO and NO<sub>2</sub>. We bin the data into monthly samples on a 4° latitude grid prior to the statistical analyses discussed below. Because HALOE does not observe polar regions during much of the year, we focus results on the latitude band 60°N-S.

The HALOE measurement approach is ideal for examining long-term changes in constituents because it uses a ratio method. Retrievals are performed on limb transmission versus height, obtained by dividing the signal observed while viewing the sun through the atmospheric limb to that measured when viewing the unattenuated solar signal (prior to or after an occultation event). This method is virtually self-calibrating in terms of systematic errors such as detector responsivity or optics throughput changes, i.e., these errors are removed by the ratio. Other instrument checks routinely performed (e.g., spectral, gas cell, pointer tracker) show no significant long-term changes. In summary, all indications from the HALOE instrument and experiment support the validity of the observed long-term changes in constituents.

### 2.2. SAGE II

Ozone and NO<sub>2</sub> observations are also available from SAGE II measurements spanning November 1984-December 1998 [McCormick *et al.*, 1989; Cunnold *et al.*, 1991]. We use here an experimental version of the v6.0 retrieval (termed v6.0b), which incorporates improved separation of constituent and aerosol effects together with improved calibration and altitude registration characteristics. Although these new data products are still undergoing scientific validation analyses, we note that the results of interest here are also evident in prior versions of SAGE II data (i.e., retrieval v5.96). Since SAGE II is a solar

occultation instrument, the space-time sampling (and our data analysis) is similar to that for HALOE.

### 2.3. Stratospheric Circulation Diagnostics

We include analyses of the long record of stratospheric temperature measurements derived from the Stratospheric Sounding Unit (SSU) on board the series of NOAA operational satellites. The time series here are monthly averages spanning the time period November 1978-May 1998. These data have been adjusted using temporal overlap between individual satellite instruments to provide homogeneous time series of stratospheric radiance measurements; they provide more temporal continuity in the middle and upper stratosphere than available using operational NMC/CPC stratospheric temperatures [e.g., Finger *et al.*, 1993]. These measurements are from the 3 original SSU channels, plus 5 additional 'synthetic' channels derived from differences between nadir and off-nadir SSU measurements [see Nash, 1988]. The radiance measurements correspond to layer mean temperatures over  $\sim 10\text{-}15$  km thick levels; the weighting functions for these temperature measurements can be found in Chapter 5 of WMO [1999]. We furthermore include some diagnostics of stratospheric eddy forcing derived from the NCEP [Kalnay *et al.*, 1996] and ECMWF [Gibson *et al.*, 1997] reanalyses, and from the NCEP/CPC stratospheric analyses [Finger *et al.*, 1993]. The estimates of interannual changes in these derived quantities are subject to some uncertainties, and we include results from these separate analyses to provide one estimate of such uncertainties.

### 2.4. Data Analyses

Our objective here is to quantify the low-frequency trend-like variability in the constituent data sets. In general these interannual changes are relatively small compared to oscillatory variations associated with the seasonal cycle and the quasi-biennial oscillation (QBO), although this statement depends on the species in question and the specific location. An example where the seasonal and QBO components are large is for  $\text{H}_2\text{O}$  in the low latitude middle stratosphere, as shown in the time series of Figure 1. For the occultation measurements we fit the seasonal cycle at each latitude and pressure using harmonic regression analysis (Figure 1a). The deseasonalized interannual anomalies (Figure 1b) show large variations with an approximate 2-year period, which are coherent with the QBO in equatorial zonal winds. A regression onto the QBO winds over 70-10 mb (using two orthogonal basis

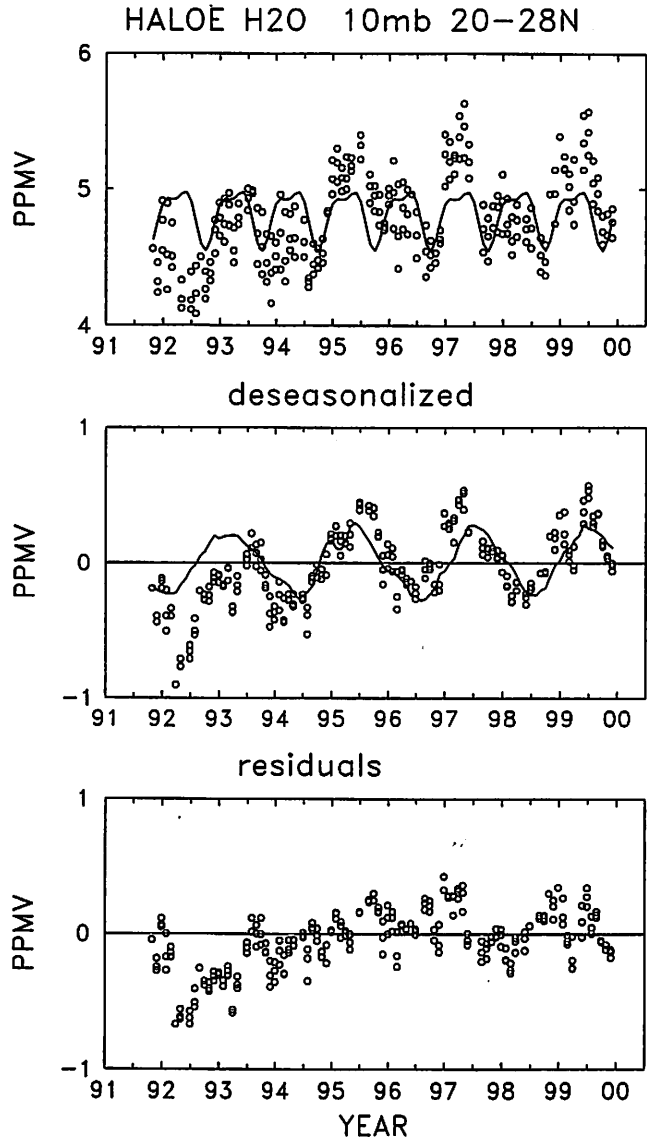


Figure 1. (top) Time series of HALOE  $\text{H}_2\text{O}$  measurements at 10 mb over 20-28°N. The solid line shows the (repeating) seasonal cycle fit. (middle) Corresponding deseasonalized  $\text{H}_2\text{O}$  anomalies, together with the QBO fit derived from regression. (bottom) Residual anomalies (deseasonalized anomalies minus the QBO fit).

functions) provides a dynamically-based accurate empirical fit of the QBO variability, as shown in Figure 1b [the details of the seasonal and QBO regression fits are discussed in Randel and Wu, 1996 and Randel *et al.*, 1998]. The residual of the QBO-fit (Figure 1c) shows the low-frequency changes of most interest for the current work:

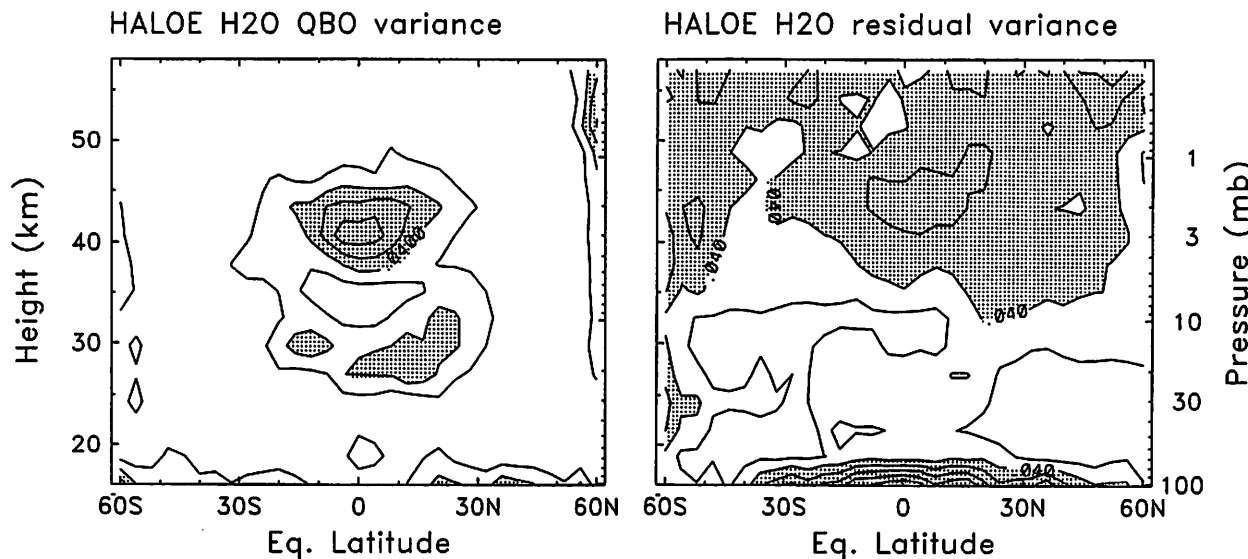


Figure 2. Meridional cross sections of interannual variance in HALOE H<sub>2</sub>O data associated with the QBO (left) and the residual (right) for data over 1991-1999. The contour interval is 0.02 ppmv<sup>2</sup>.

the H<sub>2</sub>O variations in Figure 1c show a slight increase during 1991-1995, and relatively constant values thereafter. Note that these changes are evident in the 'full' time series (Figure 1a), but are highlighted by removing the seasonal and QBO signals.

An important point is that the QBO is often a large component of variability in constituent data, and one which complicates interpretation of "other" low-frequency changes in relatively short time records. Figure 2 shows the temporal variance in HALOE H<sub>2</sub>O data during 1991-1999 associated with the QBO and with the residual interannual anomalies (calculated as in Figure 1). The distinctive equatorially-centered spatial structure of the QBO is evident in Figure 2, contrasting with the global character of the residual. Figure 2 illustrates that the relative importance of the QBO depends on the altitude and latitude region of interest; for the HALOE and SAGE II constituent data the QBO is generally large between 20-45 km and 40°N-S.

Our philosophy here is to isolate the low-frequency interannual changes in constituents using the least amount of filtering necessary. Time series of area-averaged deseasonalized anomalies illustrate the variations most simply; we remove the QBO signal for ozone and NO<sub>x</sub> variations in the middle stratosphere in some of the diagnostics below, using the regression fits described above. Anomalies averaged over each hemisphere are shown to illustrate the global character of the 'trends.' Smoothed versions of the global anomalies are derived by use of a moving Gaussian weighting, with a half-width of

15 months (roughly equivalent to 3-year running means), intended to minimize QBO effects. Although the overall variability is not linear for most species, we calculate linear trends over 5-year samples at the beginning and end of the record in order to quantify spatial structure of changes during these times. The trends are calculated by standard regression analyses, and standard errors of the statistical fits are derived using bootstrap resampling of the original anomalies [Efron and Tibshirani, 1993].

### 3. CONSTITUENT OBSERVATIONS

#### 3.1. CH<sub>4</sub> and H<sub>2</sub>O

The overall structure and variability of CH<sub>4</sub> and H<sub>2</sub>O are tightly coupled in the stratosphere, because CH<sub>4</sub> oxidation is a principal source of stratospheric H<sub>2</sub>O [e.g., Remsberg *et al.*, 1984]. The oxidation reactions produce approximately two molecules of H<sub>2</sub>O for each one of CH<sub>4</sub>; this photochemical conversion occurs as air ages in the middle and upper stratosphere, and hence anticorrelated changes in CH<sub>4</sub> and H<sub>2</sub>O signify variations in the age of air induced by transport. Empirical studies have shown the quantity  $D = H_2O + 2CH_4$  is an approximately conserved parameter throughout much of the stratosphere [Dessler *et al.*, 1994; Remsberg *et al.*, 1996], and we thus examine the variability of CH<sub>4</sub>, H<sub>2</sub>O, and H<sub>2</sub>O + 2CH<sub>4</sub>.

Figure 3 shows time series of hemispherically-averaged deseasonalized anomalies in CH<sub>4</sub>, H<sub>2</sub>O, and H<sub>2</sub>O + 2CH<sub>4</sub> near the stratopause. Included on these plots are smooth

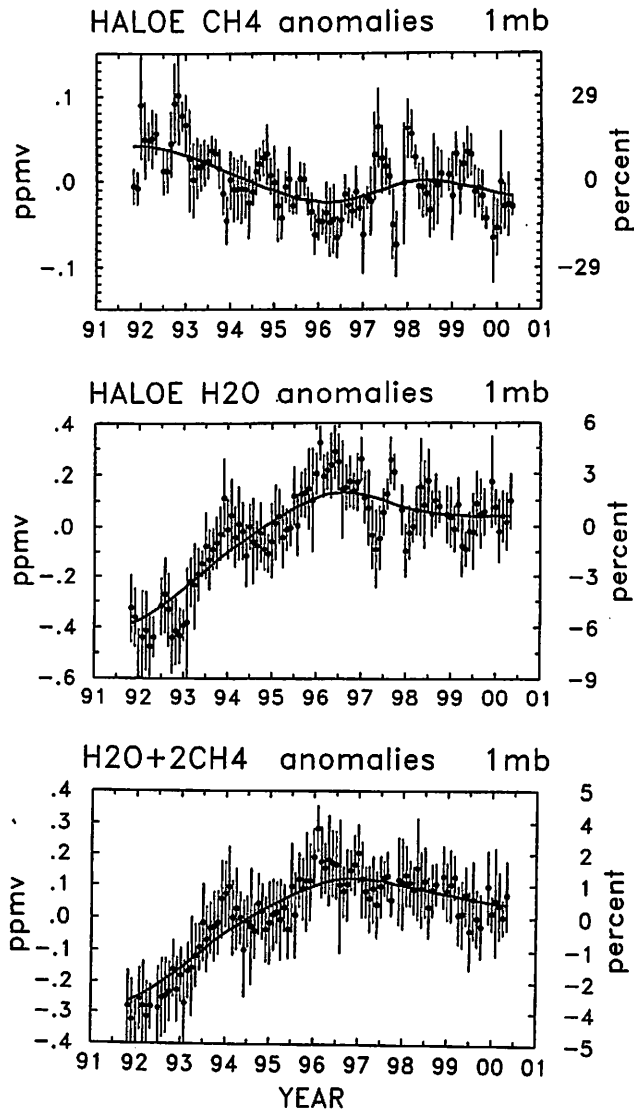


Figure 3. Time series of deseasonalized anomalies in CH<sub>4</sub> (top), H<sub>2</sub>O (middle) and H<sub>2</sub>O + 2CH<sub>4</sub> (bottom) at 1 mb (~ 48 km) derived from HALOE data. Circles denote the monthly global means, and the vertical lines show plus and minus one standard deviation of all observations about the mean. The smooth curves show a moving average of the global means. Left axes are mixing ratio units, and right axes show relative percentage changes.

curves showing the low frequency interannual variations of the corresponding global means. The CH<sub>4</sub> anomalies show a general decrease during 1991-1995, and a slight increase since 1996. Water vapor shows just the opposite low frequency changes: increases during 1991-1995, and a leveling off or slight decrease thereafter. These 1991-1995 changes correspond to the trends reported by Nedoluha *et al.* [1998a, b], Evans *et al.* [1998] and Randel *et al.* [1999], but they have clearly not continued beyond 1996. The

variable part of total hydrogen (H<sub>2</sub>O + 2CH<sub>4</sub>) shows similar behavior as H<sub>2</sub>O alone, demonstrating that variations in CH<sub>4</sub> oxidation produce only a fraction (approximately 20%) of the H<sub>2</sub>O change during 1991-1995 (i.e., there are sources of H<sub>2</sub>O variability separate from the CH<sub>4</sub> source). Note the compensating CH<sub>4</sub>-H<sub>2</sub>O deviations in 1997-1998 in Figure 3, suggestive of global transport variability on relatively fast time scales.

Time series of deseasonalized H<sub>2</sub>O + 2CH<sub>4</sub> anomalies at 31, 10 and 3 mb (near 24, 32 and 40 km, respectively), are shown in Figure 4. Each of these time series shows similar low-frequency changes as the ~ 50 km data in Figure 3, i.e., a clear increase during the first half of the HALOE record, and near-constant or slightly decreasing values thereafter. The time variations for H<sub>2</sub>O alone are similar (not shown). The global nature of the low-frequency changes, and the dramatic differences between the first half and latter half of the HALOE record, are illustrated in Figure 5, which show linear trends in H<sub>2</sub>O for the 5-year periods 1992-1996 and 1995- 1999. The positive H<sub>2</sub>O trends (of ~ 1-2% per year) seen throughout the stratosphere and lower mesosphere for the 1992-1996 period are absent (or reversed) for the period since 1995. Similar calculations for CH<sub>4</sub> (Figure 6) also reveal dramatic differences: the intriguing 1992-1996 decrease in CH<sub>4</sub> over 35-65 km is reversed or absent in the recent record. These calculations demonstrate that the interannual variations in the short HALOE record are not representative of monotonic decadal-scale trends, but rather are suggestive of episodic changes. One exception to this is the CH<sub>4</sub> increase in the lower stratosphere (~ 15-30 km), which is positive (of order ~ 0.5-1.0% per year) over the entire HALOE record (Figure 6). The slight decrease in trend magnitude in this region for the latter half of the record is consistent with the slowing of tropospheric CH<sub>4</sub> increases reported by *Slugokenky et al.*, 1998.

The largest H<sub>2</sub>O trends seen in Figure 5 occur in the upper mesosphere, over ~ 70-80 km, and correspond to 5-year changes of order ± 20-30%. *Chandra et al.* [1997] have analyzed H<sub>2</sub>O variability in HALOE data and a 2-D model, and demonstrated that large changes in the upper mesosphere are primarily due to changes in solar output (variations in solar Lyman  $\alpha$  associated with the 11-year solar cycle, cause out-of-phase changes in H<sub>2</sub>O). Figure 7 shows time series of global-mean HALOE H<sub>2</sub>O anomalies at 0.01 mb (~ 80 km), together with time series of the Lyman- $\alpha$  irradiance measured by the UARS SOLSTICE instrument [*London et al.*, 1993], showing this temporal anti-correlation. It is interesting that the overall low-frequency variations in H<sub>2</sub>O at 80 km are similar to changes

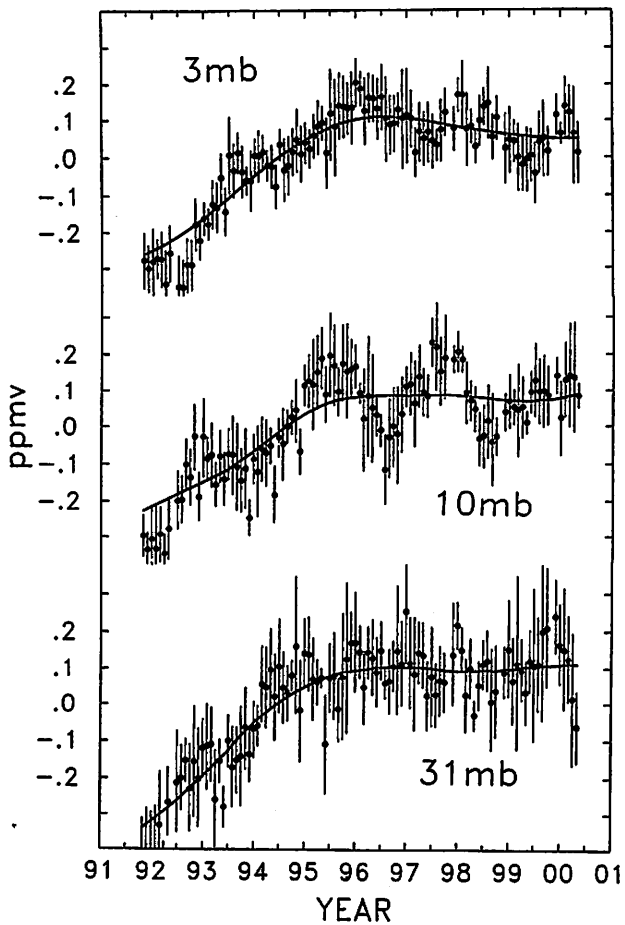


Figure 4. Time series of global anomalies in  $\text{H}_2\text{O} + 2\text{CH}_4$  at 31, 10 and 3 mb (near 24, 32 and 40 km, respectively). Details are the same as in Figure 3.

at stratospheric levels (Figures 3-4) although *Chandra et al.* [1997] suggest that direct (photochemical) solar effects are mostly important above  $\sim 70$  km (consistent with the vertical structure of largest trends seen in Figure 5).

### 3.2. HF and HCl

HF and HCl in the middle atmosphere are similar in that they both originate primarily as the photochemical breakdown products of tropospheric chlorofluorocarbons (CFC's). HF has no significant natural sources, while about 80% of stratospheric HCl originates from CFC's. Time series of HF and HCl near the stratopause are shown in Figure 8, extending the HALOE time series shown in *Russell et al.* [1996], *Considine et al.* [1997], and *WMO* [1999] and covering the same time period analyzed by *Anderson et al.* [2000]. In Figure 8 we show the full HF and HCl time series rather than deseasonalized data, in order to illustrate the magnitude of the absolute changes.

The HF measurements show a monotonic increase throughout the HALOE record, with a slowing of the trend rate after approximately 1997. The HCl time series show a clear maximum in  $\sim 1996$ -1997, with decreasing values for 1998-1999. The differing behaviors of HF and HCl are related to variations in the respective tropospheric fluorine and chlorine emissions, as demonstrated in *Anderson et al.* [2000]. The clear turnover in stratospheric HCl is associated with a similar change in tropospheric chlorine loading, which had an observed maximum in  $\sim 1993$  [Montzka et al., 1999]. The linear HCl and HF increases during 1992-1996 fit the tropospheric emissions with an approximate 5-year time lag [Russell et al., 1996; *Anderson et al.*, 2000], roughly consistent with the inferred age of air in the upper stratosphere [Hall et al., 1999]. However, the time lag between peak chlorine amounts in the troposphere ( $\sim 1993$ ) and upper stratosphere ( $\sim 1996$ -1997) is only  $\sim 3$ -4 years, and the reason for this somewhat shorter time lag (i.e., earlier turnover of HCl than expected) is not understood at present.

### 3.3. Ozone and $\text{NO}_x$

Ozone and  $\text{NO}_x$  ( $\text{NO} + \text{NO}_2$ ) are photochemically coupled in the middle atmosphere, because  $\text{NO}_x$  is the main mechanism for catalytic ozone destruction over  $\sim 25$ -40 km [e.g., *Osterman et al.*, 1997]. HALOE provides sunrise and sunset measurements of both NO and  $\text{NO}_2$ . Both constituents exhibit strong diurnal cycles, and sunset  $\text{NO}_x$  is somewhat larger than sunrise  $\text{NO}_x$  due to daytime photolysis of  $\text{N}_2\text{O}_5$  [which builds up during the night; e.g., *Neivison et al.*, 1996]. Here we analyze the sunset observations of  $\text{NO}_x$  together with ozone to demonstrate coupled variability.

Time series of ozone and  $\text{NO}_x$  anomalies at 10 mb are shown in Figure 9, and here we have removed the QBO signal together with the seasonal cycle, because the QBO is relatively large for these constituents in the middle stratosphere [Randel et al., 1996]. The month-to-month variability in these constituents appears significantly larger than that observed in the longer lived species  $\text{H}_2\text{O}$ ,  $\text{CH}_4$ , HF and HCl (Figures 3, 4 and 8). In terms of low frequency changes, ozone shows a gradual decline over  $\sim 1991$ -1996, coincident with increasing  $\text{NO}_x$ , while both quantities are relatively constant since  $\sim 1996$ . The spatial structure of the anti-correlated ozone- $\text{NO}_x$  changes over 1992-1996 are illustrated by the linear trends shown in Figure 10. Ozone trends show a decrease in the tropical middle stratosphere over  $\sim 30$ -40 km, while  $\text{NO}_x$  shows an increase everywhere below  $\sim 40$  km and decreases over 40-50 km (note the spatially coincident maxima seen in  $\text{O}_3$  and

$\text{NO}_x$  trends near 35 km). Ozone and  $\text{NO}_x$  trends for the period 1995-1999 (not shown) exhibit almost no significant values (e.g., Figure 9), so that the changes in the early HALOE record were not characteristic of longer-term (decadal) trends. This is also consistent with the fact that the 1992-1996 ozone trends (Figure 10) are completely different from the ~ 15-20 year ozone trends derived from SAGE or SBUV satellite data [see WMO, 1999], which exhibit no significant trends in the tropical middle stratosphere (as shown below). Two other aspects of interest in Figure 10 are (1) increases in tropical ozone near ~ 25 km, and (2) near-global  $\text{NO}_x$  decreases over ~ 40-50 km. The latter is due almost entirely to decreases in NO, as  $\text{NO}_2$  contributes little to  $\text{NO}_x$  above 40 km.

A longer-term perspective of recent ozone and  $\text{NO}_2$  variability is provided by SAGE II observations spanning 1984-present. SAGE II does not measure NO, so we focus on variability of  $\text{NO}_2$  in comparisons with HALOE. Figure 11 show time series of anomalies in tropical ozone at 10 mb (~ 32 km), and  $\text{NO}_2$  at 15 mb (~ 30 km) for both SAGE II and HALOE measurements. Here we have removed the respective QBO variations, which are relatively large for ozone and  $\text{NO}_2$  in this region [Randel and Wu, 1996]. This comparison shows reasonable overall agreement between the HALOE and SAGE II data during 1992-1998, and in particular the low-frequency changes seen in HALOE data over ~ 1991-1995 (decreases in ozone and increases in  $\text{NO}_2$ ) are also evident in the SAGE II results. However, the longer-term perspective of SAGE II observations suggests that the changes during this time period were anomalous and not representative of decadal-scale trends. Rather, the close association with the Pinatubo eruption suggests volcanic effects as a likely causal mechanism, although some substantial low-frequency changes also occur in the SAGE II data prior to Pinatubo (note the anti-correlated ozone- $\text{NO}_2$  variations during 1988-1990). Overall the HALOE-SAGE II agreement and the coherent changes in ozone and  $\text{NO}_2$  are strongly suggestive of true atmospheric variability (as opposed to instrumental artifacts).

To further emphasize the variability of short-term 'trends,' Figure 12 compares SAGE II ozone trends for the short period 1992-1996 versus those calculated for 1984-1998. The 1992-1996 trends show largest changes in the tropics, with decreases over ~ 30-45 km and increases near 25 km; the spatial patterns and magnitudes are very similar to the HALOE results in Figure 10. In contrast, the 14-year SAGE II trends in Figure 12 are completely different, with significant negative trends only in the extratropical upper stratosphere, and small changes in the tropics. This clearly demonstrates that observed changes for the several years following Mt. Pinatubo do not reflect decadal-scale variations in the stratosphere.

#### 4. STRATOSPHERIC TEMPERATURE AND CIRCULATION CHANGES

The observed low-frequency variations seen in the constituent data sets (particularly the long-lived  $\text{CH}_4$  and  $\text{H}_2\text{O}$  data) are suggestive of possible changes in stratospheric circulation: higher  $\text{CH}_4$  near the stratopause can be a signature of enhanced tropical upwelling (bringing up photochemically 'younger' air with relatively more  $\text{CH}_4$ ). Such variations in stratospheric circulation could result from the Pinatubo volcanic eruption in 1991 [Nedoluha *et al.*, 1998b], or from changes due to solar forcing, tropospheric wave driving of the stratosphere, or internal dynamic variability. The relative magnitudes of interannual variations in mean or eddy transport circulations associated with these different processes is poorly known at present, because such circulations are difficult to diagnose from observed or assimilated circulation statistics, particularly for small interannual variations. A more simplified and qualitative approach is to examine circulation statistics which are related to the strength of the mean stratospheric Brewer-Dobson circulation. Here we examine stratospheric temperature anomalies, which are indicative of circulation changes on the global scale. A second diagnostic of interannual changes in the mean circulation is provided by estimates of the tropospheric planetary wave forcing, as quantified in meteorological analyses (discussed below).

Time series of global mean temperature anomalies spanning the lower to upper stratosphere are shown in Figure 13. These are an update of the stratospheric temperature time series shown in WMO [1999]. Apparent in these data are (1) episodic warming in the lower-middle stratosphere for the El Chichon (1982) and Pinatubo (1991) volcanic eruptions, (2) significant long-term cooling, particularly in the upper stratosphere, and (3) an 11-year solar signal in the middle and upper stratosphere (which together with the negative trend produces a 'stair-step' variation near 42 km in Figure 13). The spatial structure of trends and solar cycle variations in the SSU temperature data are illustrated in Figure 14, with the solar component calculated by regression onto a smoothed F10.7-cm solar radio flux time series. These results are similar to those shown in Chapter 5 of WMO [1999], but updated using data through 1979-1998. Significant negative trends are observed over much of the stratosphere, with largest values (approximately -2 K/decade) near the stratopause. The solar variations in the data are largest in the tropical middle and upper stratosphere, with approximately 1 K variations between solar minimum and maximum. The mean Brewer-Dobson circulation changes associated with the trend and solar cycle variations in the stratosphere have yet to be quantified, but are an important topic for future study.

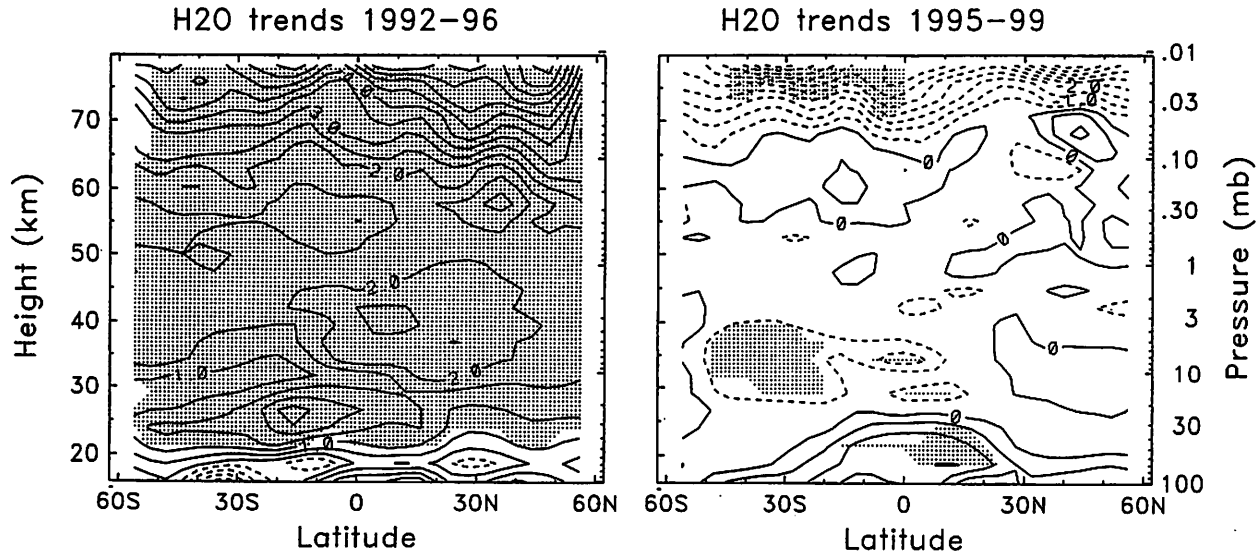


**Figure 5.** Meridional cross section of linear trends in HALOE H<sub>2</sub>O measurements for the period 1992-1996 (left) and 1995-1999 (right). Contours interval is 0.5% per year in both panels; shaded areas indicate statistically significant trends.

The volcanic eruptions of El Chichon and Pinatubo produce strong global mean warmings that last for 1-2 years (Figure 13). The spatial structure of the temperature anomalies in SSU data following the Pinatubo eruption are shown in Figure 15; these are calculated as average anomalies for one year following the eruption (July 1991-June 1992), with prior statistical removal of the trend, solar and QBO temperature signals. Shaded regions in Figure 15 show where the temperature anomalies are statistically significant, in the sense of being larger than twice the local standard deviation of annual mean anomalies over 1979-1997 (a measure of 'natural' variability of annual means). These temperature anomaly patterns show a warming of the lower stratosphere below  $\sim 27$  km over much of the globe, with maxima in the tropics of  $\sim 1.5$  K. The maximum lower stratospheric warming was probably in excess of 3 K [Labitzke and McCormick, 1992], but this signal is less in the thick layer SSU temperatures. In the middle and upper stratosphere, significant warm anomalies are observed in extratropics of each hemisphere, with relative cooling in the tropics. There is a good deal of global symmetry in the patterns in Figure 15, and although the magnitudes of the anomalies are not large, their persistence for an entire year is remarkable. Although not shown here, overall similar anomalies are found for the year following the El Chichon eruption in 1982.

Included in the Pinatubo results in Figure 15 are arrows indicating (qualitatively) the mean meridional circulation anomalies which would be in balance with the upper stratospheric temperature patterns [see Andrews *et al.*, 1987]. These show sinking motion in high latitudes of both

hemispheres and, by continuity, anomalous upwelling in the tropics. Calculated model results [e.g., Brasseur and Granier, 1992; Rosenfield *et al.*, 1997] and diagnostic analyses [Eluszkiewicz *et al.*, 1997] of the Pinatubo tropical circulation following the Pinatubo eruption show upward circulation anomalies also in the tropical lower stratosphere; the direct aerosol radiative heating (between  $\sim 15$ -30 km) results in local warming (as in Figure 15) plus induced upward motion. Hence the inferred global circulation anomalies for the year following the Pinatubo eruption are upward in the tropics throughout the entire stratosphere, with compensating downward motion over both NH and SH extratropics. This enhanced tropical upwelling is qualitatively consistent with the relatively high CH<sub>4</sub> anomalies during 1992-1993 seen in Figure 3.

A fundamental driver of the stratospheric circulation is the vertical flux of planetary wave activity from the troposphere into the winter stratosphere [Andrews *et al.*, 1987; Haynes *et al.*, 1991; Holton *et al.*, 1995]. Interannual variations in wave forcing should therefore be reflected in changes in mean circulation; analyses of wave forcing diagnostics are thus complementary to studies of global temperature variability. A concise diagnostic for the amount of planetary wave forcing from the troposphere into the stratosphere is given by the vertical component of the Eliassen-Palm (EP) flux in the lower stratosphere, which is proportional to the zonal mean eddy heat flux  $\bar{v}T$  [Andrews *et al.*, 1987]. Figure 16 shows time series of winter-mean (November-March) eddy heat flux in the NH (averaged over 40-70°N at 100 mb), for the years 1979-1999 (1979=November 1978 to March 1979). Three

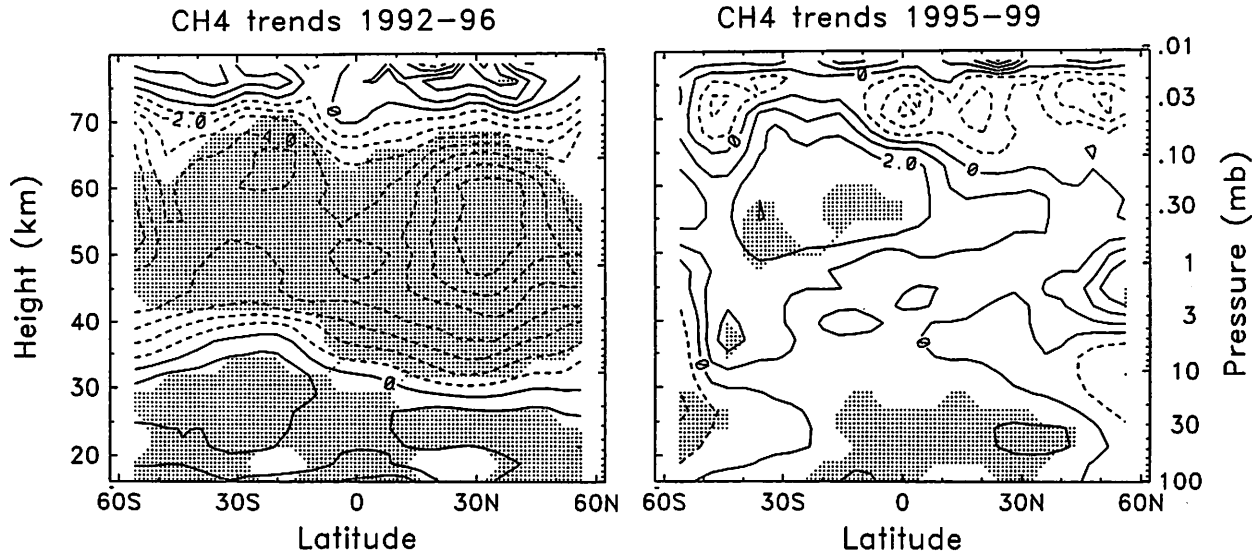


Figure 6. Linear trends in HALOE CH<sub>4</sub> measurements for the periods 1992-1996 (left) and 1995-1999 (right). Contour interval is 1% per year.

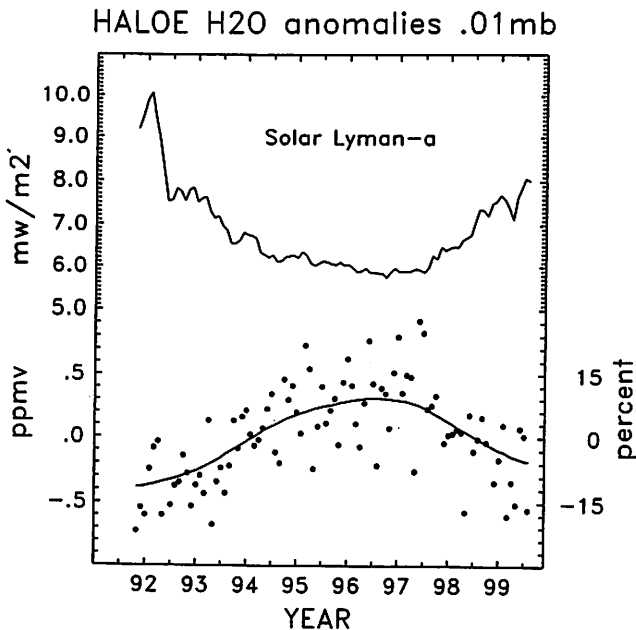


Figure 7. Time series of global anomalies in HALOE H<sub>2</sub>O at 0.01 mb (~80 km), together with variability of the solar Lyman- $\alpha$  flux measured by the SOLSTICE instrument on UARS.

separate estimates of  $\sqrt{vT}$  are shown in Figure 16, derived from NCEP and ECMWF reanalyses and Climate Prediction Center (CPC) stratospheric analyses; these give slightly different results which provide one estimate of the uncertainty in this derived quantity (see Newman and Nash, 2000, for detailed discussion). The time series in Figure 16 show interannual variations in wave forcing of up to  $\sim \pm$

15% for the winter mean. Of particular note is the relative minimum in wave forcing for the years 1993-1997, compared to the pre-1990 mean; this minimum is somewhat accentuated in the CPC results. This reduced wave driving can result in a weakened Brewer-Dobson circulation (reduced tropical upwelling), which could be reflected in the relatively low CH<sub>4</sub> anomalies during ~ 1994-1997 seen in Figure 3. Furthermore, the increased wave forcing during 1998-1999 seen in Figure 16 could by this mechanism account for the increased CH<sub>4</sub> observed during this period in Figure 3. However, these arguments are qualitative, and detailed modeling studies are probably required to isolate tropospheric forcing effects from volcanic, solar or other mechanisms.

## 5. SYNTHESIS AND DISCUSSION

Beyond the seasonal cycle and QBO variations, the most obvious characteristic of the HALOE constituent data are a change in low-frequency interannual 'trends.' The remarkable increases in H<sub>2</sub>O throughout the stratosphere, and decreases in CH<sub>4</sub> in the upper stratosphere-lower mesosphere, seen in the early HALOE record have not continued beyond ~ 1996 (and partially reverse in 1998-1999). In fact, there are virtually no significant trends in the H<sub>2</sub>O and CH<sub>4</sub> data over the period 1995-1999 (except for increases in CH<sub>4</sub> in the lower stratosphere). Similar temporal variability is observed in HALOE measurements of ozone and NO<sub>x</sub>, i.e., a flattening of 'trends' apparent in the early record. The longer term perspective of SAGE II

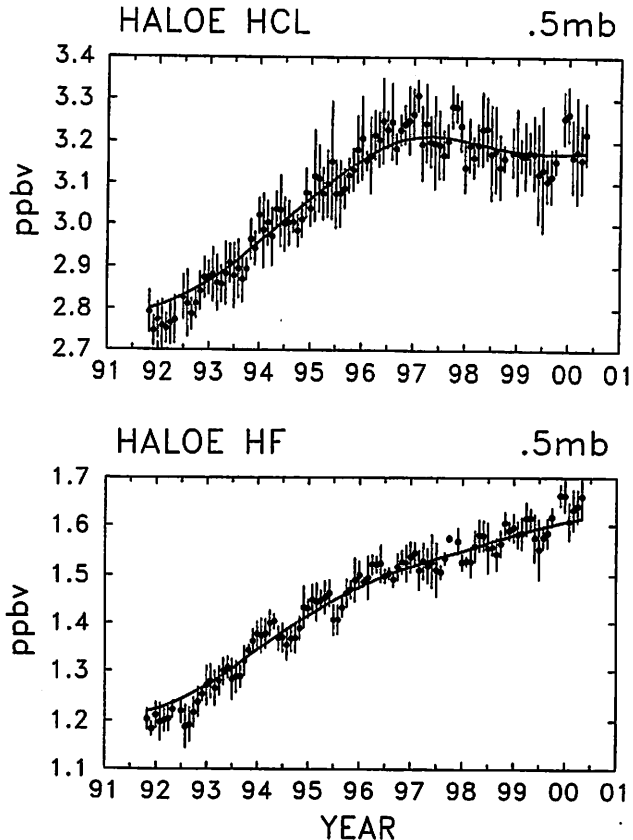


Figure 8. Time series of global variations in HALOE HCl (top) and HF (bottom) at 0.5 mb (~ 53 km). Note these data are not deseasonalized. Details are the same as Figure 3.

data demonstrates that the ozone and NO<sub>2</sub> changes over ~ 1992-1996 are not characteristic of decadal-scale variations, but are more episodic in character. One possibility is that these constituent variations reflect a prolonged recovery from the Mt. Pinatubo eruption in 1991, since more recent data exhibit values similar to pre-Pinatubo averages. HF is the only stratospheric constituent measured by HALOE that continues to increase after 1997. HCl decreases after this time, which is evidence for the atmospheric response to the Montreal Protocol regulations [Anderson *et al.*, 2000].

It is reasonable to question the reality of the interannual constituent changes found in HALOE data, particularly for CH<sub>4</sub> and H<sub>2</sub>O where other global measurements are unavailable. There are several aspects of these data which suggest that the changes discussed here are real. First, careful analyses of instrument stability over time show no obvious problems that would translate into spurious constituent trends. Second, there is substantial coherence in both space and time for variations in the separate HALOE constituents (e.g., the CH<sub>4</sub>, H<sub>2</sub>O, ozone and NO<sub>x</sub> all show

similar low frequency temporal changes). Third, there is overall good agreement between the HALOE and SAGE II ozone and NO<sub>2</sub> variations during 1991-1998. Also, the increases in HALOE H<sub>2</sub>O over the early record (1991-1996) were confirmed in ground-based remote sensing measurements in both hemispheres [Nedoluha *et al.*, 1998a]. Thus there are good reasons to believe the overall patterns of variability seen in the HALOE measurements. However, an important point is that 'trends' derived from short time records, with arbitrary starting and ending points, are not representative of decadal-scale change. Thus interpretation of trend-like changes in the HALOE data is a continuing question at this point.

The upper stratospheric CH<sub>4</sub> and NO<sub>x</sub> changes suggest interannual variations in the global stratospheric circulation. Pinatubo is one mechanism for such variability in the UARS time frame, together with interannual changes in tropospheric wave forcing or solar cycle effects. An increase in tropical upwelling (say, during 1991-1992) will produce 'younger' air in the upper stratosphere, with correspondingly more CH<sub>4</sub> and less H<sub>2</sub>O, qualitatively

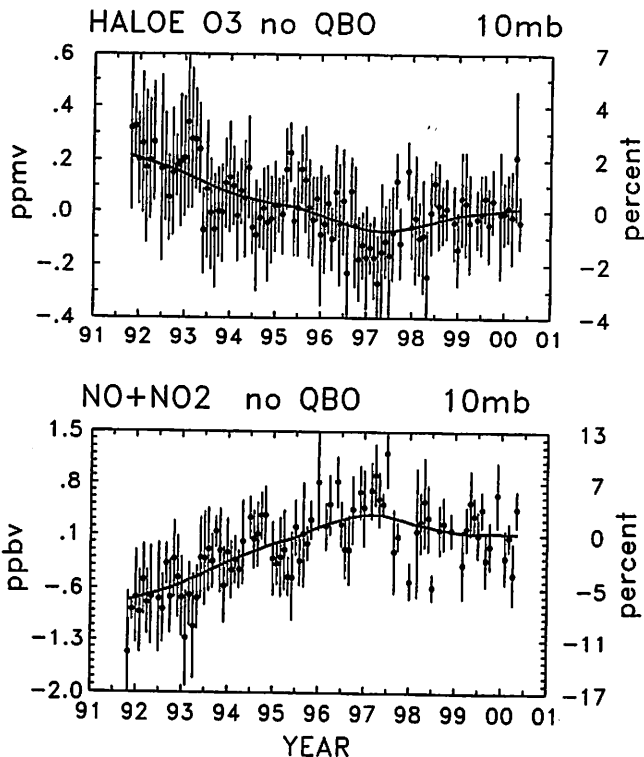


Figure 9. Time series of global anomalies in HALOE ozone (top) and sunset NO<sub>x</sub> (NO + NO<sub>2</sub>) (bottom) at 10 mb (~ 32 km). These time series have the seasonal and QBO variations removed. Details are the same as in Figure 3.

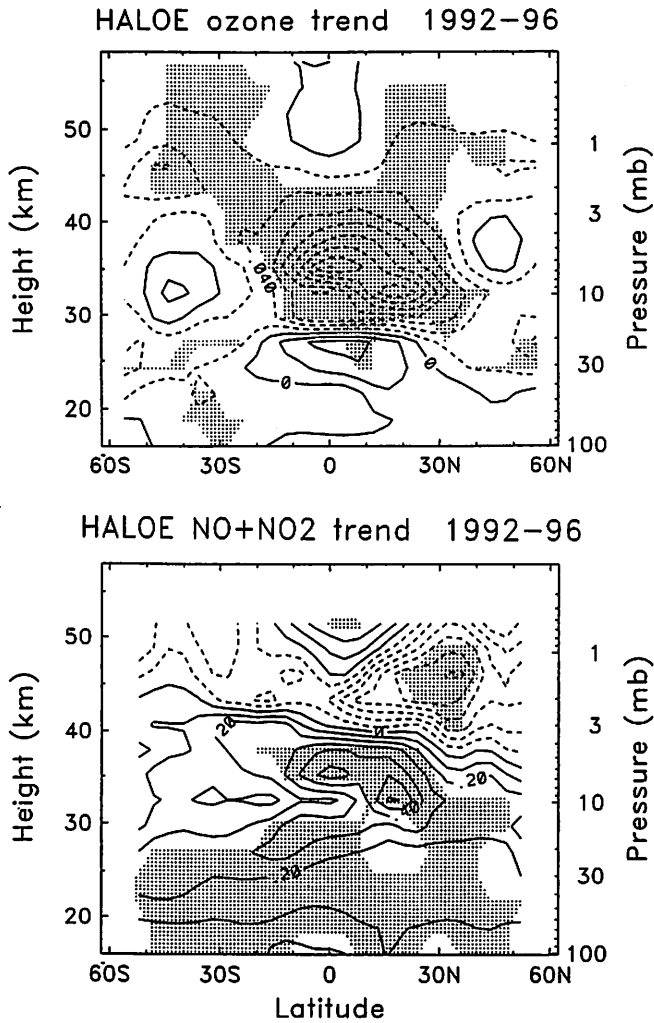


Figure 10. Cross sections of linear trends over 1992-1996 for HALOE ozone (top) and sunset NO<sub>x</sub> (NO + NO<sub>2</sub>) (bottom). Contour intervals are 0.02 ppmv/year and 0.10 ppbv/year, respectively.

consistent with Figure 3. It is also consistent with the vertical and temporal structure of NO<sub>x</sub> changes in Figure 10-11, i.e., younger air has less NO<sub>x</sub> below  $\sim 40$  km and more above this altitude, so that an equilibration to "background" conditions can produce the NO<sub>x</sub> 'trends' in Figure 10. However, aerosol-induced chemical changes also act to decrease stratospheric NO<sub>x</sub> [see for example the model calculations of Rosenfield *et al.*, 1997], so that the decrease below 40 km immediately after Pinatubo (see Figure 11) may be a mixed dynamical-chemical response. The presence of oppositely-signed NO<sub>x</sub> changes above 40 km (where chemical aerosol effects are small) argue for at least some component of a dynamical change. Presumably,

ozone in the middle stratosphere ( $\sim 30$ -40 km) responds to the NO<sub>x</sub> changes (as evidenced by the high spatial anti-correlation of trends in Figure 10).

Long records of stratospheric temperature measurements show an impulsive response to Pinatubo with equilibration in  $\sim 2$  years (to an apparently different background, i.e., Figure 13). The Pinatubo temperature anomalies are warm in the lower stratosphere over most of the globe, but only over the extratropics in the upper stratosphere (with slight cooling of the tropical upper stratosphere). The associated mean meridional circulation anomalies are suggested to be upward throughout the depth of the stratosphere in the tropics, with compensating

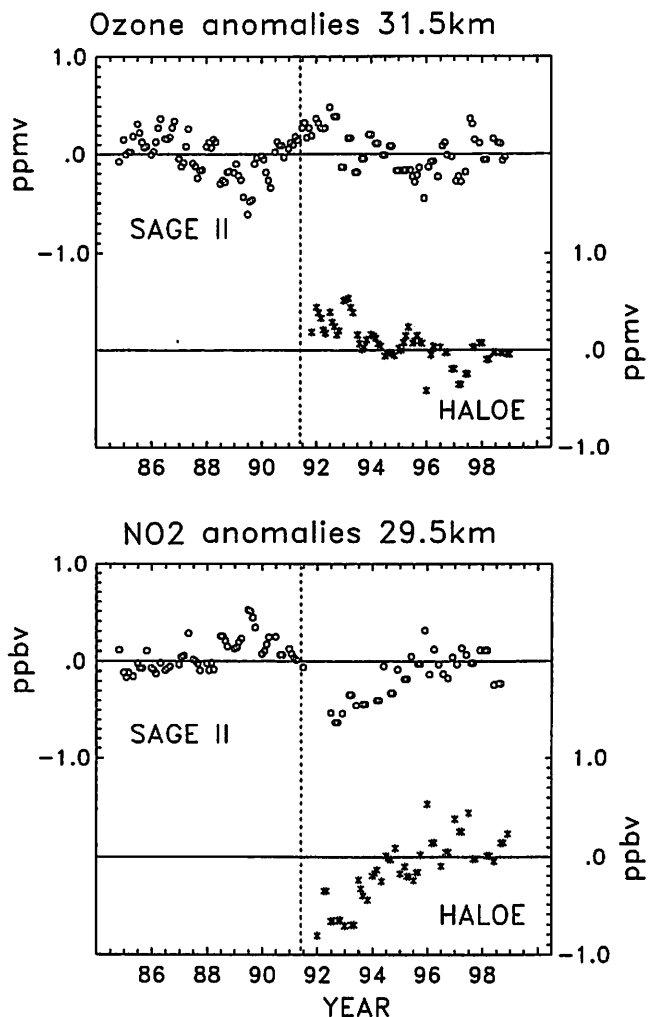


Figure 11. Time series of SAGE II and HALOE anomalies in ozone at 10 mb (top) and NO<sub>2</sub> at 15 mb (bottom). These data are averages over 20°N-20°S. The dashed lines indicate the eruption of Mt. Pinatubo (June 1991).

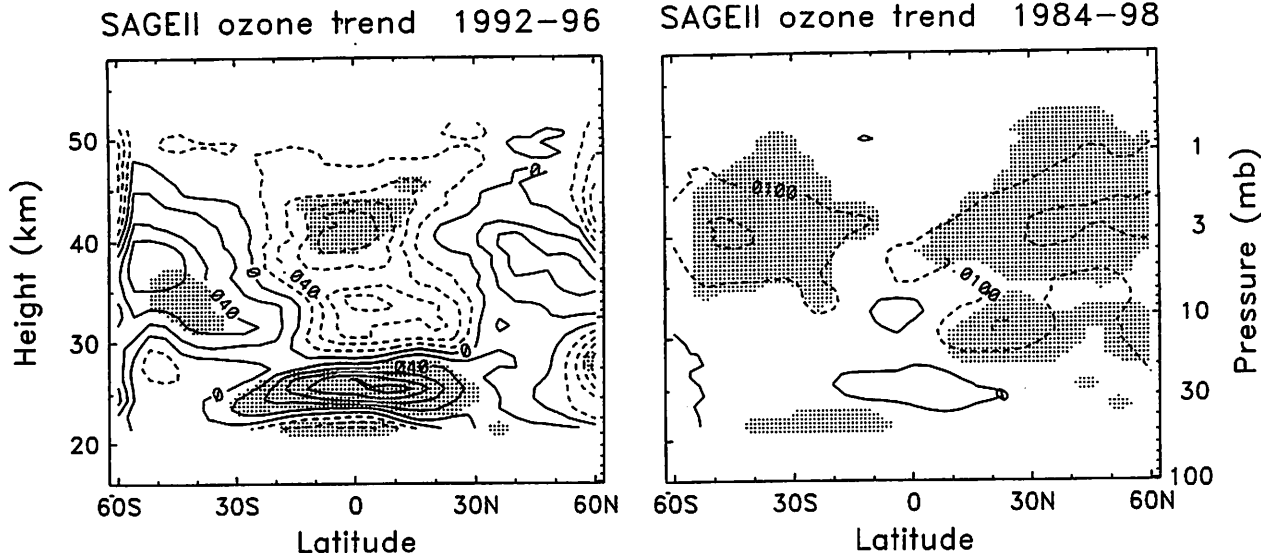
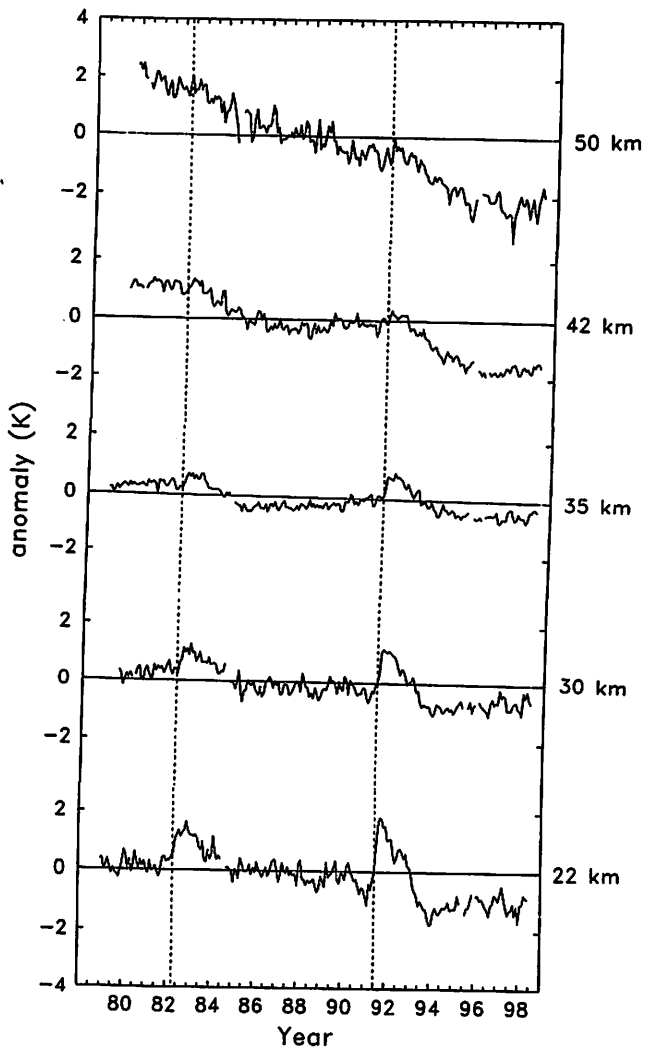


Figure 12. Trends in ozone density derived from SAGE II data for 1992-1996 (left) and 1984-1998 (right). The contour interval for 1984-1998 is half that for 1992-1996.



downward flow over extratropics (Figure 15), and this represents a strengthening of the time-mean Brewer-Dobson circulation. We note that the radiative effects of enhanced tropical ozone in the middle and upper stratosphere (seen in Figure 11) could furthermore strengthen the tropical upwelling after Pinatubo. An analysis of NH winter tropospheric wave forcing of the stratosphere (Figure 16) shows substantial year-to-year variability, but the middle 1990's are remarkable for a series of years with relatively weak forcing, which could translate into a weakened Brewer-Dobson circulation. This would give the same sense of circulation changes as that inferred from the Pinatubo temperature signal alone, i.e., a weakened circulation after 1993. We have not attempted to directly estimate anomalies in the stratospheric Brewer-Dobson circulation, but note here that modest changes in tropical upwelling in idealized models can significantly impact CH<sub>4</sub> near the stratopause [D. Waugh, personal communication, 1999].

One further factor for low-frequency variability of CH<sub>4</sub> near the stratopause is the photochemical loss associated with chlorine, which accounts for ~ 1/3 of the calculated total loss at these altitudes [C. Granier, personal communication 1997; Lary and Toumi, 1997]. The observed changes in HALOE HCl near the stratopause

Figure 13. Time series of global temperature anomalies derived from several SSU channels (from bottom to top, channels 15x, 26x, 26, 27 and 47x, respectively). Each time series provides an estimate of the temperature in a ~ 10-15 km layer, centered near the altitudes indicated at right. Dashed lines indicate the eruptions of El Chichon and Pinatubo.

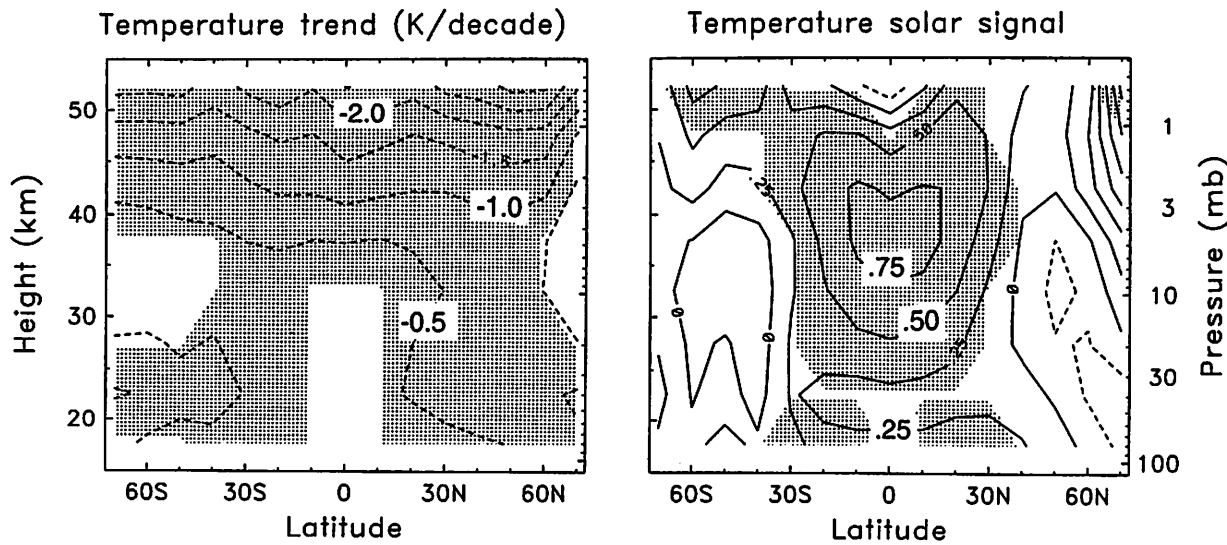


Figure 14. Spatial patterns of the trend (left, contours of 0.5 K/decade) and solar cycle variation (right, contours of 0.25 K/100 units of F10.7 solar radio flux) derived from SSU data for 1979-1998. Solar maximum-solar minimum variations of F10.7 are of order 130 units, so the solar cycle temperature changes are of order 1 K. Shading in each figure denotes a statistically significant signal.

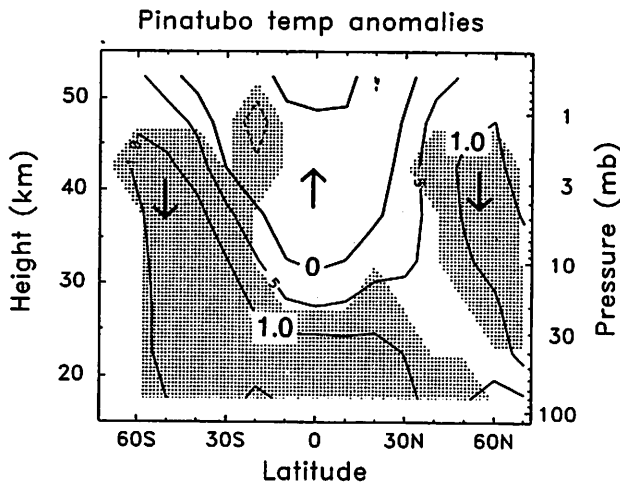
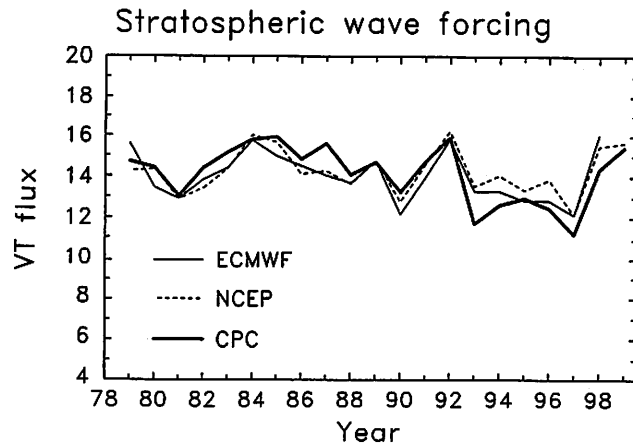


Figure 15. Cross sections of SSU temperature anomalies for the year following the Mt. Pinatubo eruption (July 1991-June 1992). Shaded regions denote where the anomalies are statistically significant as compared to 'natural' variability (as discussed in the text). Arrows in the upper stratosphere denote the sense of the associated anomalies in meridional circulation.

(Figure 8) are indicative of chlorine variations which influence CH<sub>4</sub>. The observed HCl maximum in 1996-1997 is nearly coincident with the CH<sub>4</sub> minimum, and the slight increase in CH<sub>4</sub> during 1998-1999 (Figure 3) occurs when HCl is decreasing. The influence of these chlorine changes may contribute to circulation variability in explaining the CH<sub>4</sub> 'trends'.

An outstanding problem not addressed by this change in stratospheric circulation is the source of the H<sub>2</sub>O variability not accounted for by CH<sub>4</sub> changes (i.e., the H<sub>2</sub>O + 2CH<sub>4</sub> changes seen in Figures 3-4). In light of the episodic changes in other constituents observed here, one possibility is that stratospheric H<sub>2</sub>O + 2CH<sub>4</sub> was anomalously low for the period 1991-1993, and the early HALOE trends represent a return to equilibrium. The first place to look for the cause of such anomalies is near the source region for stratospheric H<sub>2</sub>O, i.e., near the tropical tropopause [as suggested by Nedoluha *et al.*, 1998a]. Figure 17 shows time series of tropical tropopause temperature anomalies over 1979-1997 derived from global radiosonde measurements [from Randel *et al.*, 2000]. These data show near constant or decreasing temperatures during the period of increasing HALOE H<sub>2</sub>O + 2CH<sub>4</sub> (~ 1991-1995), and overall similar results are derived from NCEP or ECMWF reanalysis tropopause statistics [Randel *et al.*, 2000]. This demonstrates that the source of the early HALOE 'trends' in H<sub>2</sub>O (or anomalously low values in ~ 1991-1993) was not the large-scale mean tropopause temperature. This forces the search for causes of H<sub>2</sub>O + 2CH<sub>4</sub> variability to more subtle changes in transport across the tropopause, or to sources which are internal to the stratosphere.

The similarity of H<sub>2</sub>O variability throughout the stratosphere with the (much larger) changes near 80 km (compare Figures 3, 4 and 7) is possibly suggestive of a solar cycle influence below the mesosphere. However, the detailed calculations of Chandra *et al.* [1997] suggest that



**Figure 16.** Time series of winter mean (November–March) zonal mean eddy heat flux over 40–70°N at 100 mb. This quantity is proportional to the vertical wave activity flux from the troposphere to the stratosphere. Results are shown from calculations based on NCEP and ECMWF reanalyses and CPC stratospheric analyses.

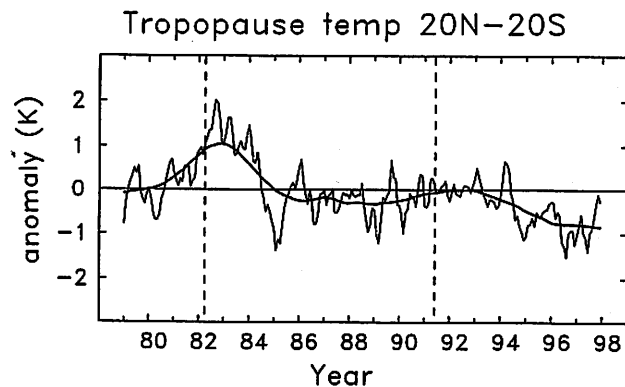


**Figure 17.** Time series of tropical tropopause temperature anomalies over 1979–1999, derived from an ensemble of tropical radiosonde measurements. Dashed lines indicate the El Chichon and Pinatubo eruptions. From Randel *et al.* [2000].

direct (photochemical) solar effects on  $\text{H}_2\text{O}$  are relatively small below  $\sim 60$  km. The fact that the upper stratospheric  $\text{CH}_4$  variations (Figure 3) show temporal changes qualitatively similar to the solar cycle (Figure 7) is also intriguing. One possibility is that solar variability could cause small changes in stratospheric circulation which contribute to transport effects. This could be of importance as well for other species which are chemically linked to  $\text{CH}_4$  [Siskind *et al.*, 1998]. It may take a long time series of measurements (at least through the current solar maximum) to empirically separate the direct effects of solar variability.

The continuing observations of stratospheric constituents by HALOE and SAGE II provide an ever changing

perspective of interannual variability in the stratosphere. We can anticipate further understanding as observations extend through the current solar cycle, and into the next decade.

**Acknowledgments.** We acknowledge support from NASA under the Atmospheric Chemistry Modeling and Analysis Program and the UARS Guest Investigator Program. We gratefully acknowledge insightful discussions and comments from Rolando Garcia, Jim Holton, Doug Kinnison, David Considine, Arun Gopalan and two anonymous reviewers. Marilena Stone expertly prepared the manuscript. NCAR is sponsored by the National Science Foundation.

## REFERENCES

Anderson, J., J. M. Russell, S. Solomon, and L. Deaver, HALOE confirmation of stratospheric chlorine decreases in accordance with the Montreal Protocol, *J. Geophys. Res.*, in press, 2000.

Andrews, D. G., J. R. Holton, and C. B. Leovy, *Middle Atmosphere Dynamics*. Academic Press, 489 pp., 1987.

Brasseur, G., and C. Granier, Mount Pinatubo aerosols, chlorofluorocarbons, and ozone depletion, *Science*, 257, 1239–1242, 1992.

Chandra, S., C. H. Jackman, E. L. Fleming, and J. M. Russell III, The seasonal and long term changes in mesospheric water vapor, *Geophys. Res. Lett.*, 24, 639–642, 1997.

Considine, G. D., L. Deaver, E. E. Remsberg, and J. M. Russell III, HALOE observations of a slowdown in the rate of increase of HF in the lower mesosphere, *Geophys. Res. Lett.*, 24, 3217–3220, 1997.

Cunnold, D., H. J. Wang, L. Thomason, J. Zawodny, and J. Logan, SAGE (v5.96) ozone trends in the lower stratosphere, *J. Geophys. Res.*, in press, 1999.

Cunnold, D. M., et al., Validation of SAGE II  $\text{NO}_2$  measurements, *J. Geophys. Res.*, 96, 12,913–12,925, 1991.

Dessler, A. E., E. M. Weinstock, E. J. Hintsa, J. G. Anderson, C. R. Webster, R. D. May, J. W. Elkins, and G. S. Dutton, An examination of the total hydrogen budget of the lower stratosphere, *Geophys. Res. Lett.*, 21, 2563–2566, 1994.

Slugocky, E. J., K. A. Masarie, P. M. Lang, and P. P. Tans, Continuing decline in the growth rate of atmospheric methane burden, *Nature*, 393, 447–450, 1998.

Efron, B., and R. J. Tibshirani, *An Introduction to the Bootstrap*, vol. 57, *Monographs on Statistics and Applied Probability*, 436 pp., Chapman and Hall, New York, 1993.

Eluszkiewicz, J., D. Crisp, R. G. Grainger, A. Lambert, A. Roche, J. Kumer, and J. Mergenthaler, Sensitivity of the residual circulation diagnosed from UARS data to the uncertainties in the input fields and to the inclusion of aerosols, *J. Atmos. Sci.*, 54, 1739–1757, 1997.

Evans, S. J., R. Toumi, J. E. Harries, M. P. Chipperfield, and J. M. Russell III, Trends in stratospheric humidity and the sensitivity of ozone to these trends, *J. Geophys. Res.*, 103, 8715–8725, 1998.

Finger, F. G., M. E. Gelman, J. D. Wild, M. L. Chanin, A. Hauchecorne, and A. J. Miller, Evaluation of NMC upper-

stratospheric temperature analyses using rocketsonde and lidar data, *Bull. Am. Meteorol. Soc.*, 24, 789-799, 1993.

Froidevaux, L., et al., Variations in the free chlorine content of the stratosphere (1991-1997): Anthropogenic volcanic and methane influences, *J. Geophys. Res.*, in press, 2000.

Gibson, J. K., P. Kallberg, S. Uppala, A. Hernandez, A. Nomura, and E. Serrano, *ERA Description. ECMWF re-analysis project Report No. 1*, Reading, UK, 1997.

Hall, T. M., D. W. Waugh, K. A. Boering, and R. A. Plumb, Evaluation of transport in stratospheric models, *J. Geophys. Res.*, 104, 18,815-18,839, 1999.

Hamilton, K., Free and forced interannual variability of the circulation in the extratropical northern hemisphere middle atmosphere, 2000, this volume.

Haynes, P. H., C. J. Marks, M. E. McIntyre, T. G. Shepherd, and K. P. Shine, On the 'downward control' of extratropical diabatic circulation by eddy-induced zonal mean forces, *J. Atmos. Sci.*, 48, 651-678, 1991.

Holton, J. R., P. H. Haynes, M. E. McIntyre, A. R. Douglass, R. B. Rood, and L. Pfister, Stratosphere-troposphere exchange, *Rev. Geophys.*, 33, 403-439, 1995.

Kalnay, E., et al., The NCEP/NCAR 40-year reanalysis project, *Bull. Am. Met. Soc.*, 77, 437-471, 1996.

Labitzke, K., and M. P. McCormick, Stratospheric temperature increases due to Pinatubo aerosols, *Geophys. Res. Lett.*, 19, 207-210, 1992.

Lary, D. J., and R. Toumi, Halogen catalyzed methane oxidation, *J. Geophys. Res.*, 102, 23,421-23,428, need a year.

London, J., G. Rottman, T. Woods, and F. Wu, Time variations of solar UV irradiance as measured by the SOLSTICE (UARS) instrument, *Geophys. Res. Lett.*, 20, 1315-1318, 1993.

McCormick, M. P., J. M. Zawodny, R. E. Viega, J. C. Larsen, and P. H. Wang, An overview of SAGE I and II ozone measurements, *Planet. Space Sci.*, 37, 1567-1586, 1989.

Montzka, S., et al., Present and future trends in the atmospheric burden of ozone-depleting halogens, *Nature*, 398, 690-694, 1999.

Nash, J., Extension of explicit radiance observations by the stratospheric sounding unit into the lower stratosphere and lower mesosphere, *Quart. J. Roy. Meteor. Soc.*, 114, 1153-1171, 1988.

Nedoluha, G. E., R. M. Bevilacqua, R. M. Gomoz, D. E. Siskind, and B. C. Hicks, Increases in middle atmospheric water vapor as observed by the Halogen Occultation Experiment and the ground-based Water Vapor Millimeter-Wave Spectrometer from 1991 to 1997, *J. Geophys. Res.*, 103, 3531-3543, 1998a.

Nedoluha, G. E., D. E. Siskind, J. T. Bacmeister, R. M. Bevilacqua, and J. M. Russell III, Changes in upper stratospheric  $\text{CH}_4$  and  $\text{NO}_2$  as measured by HALOE and implications for changes in transport, *Geophys. Res. Lett.*, 25, 987-990, 1998b.

Neivison, C. D., S. Solomon, and J. M. Russell III, Nighttime formation of  $\text{N}_2\text{O}_5$  inferred from Halogen Occultation Experiment sunrise/sunset  $\text{NO}_x$  ratios, *J. Geophys. Res.*, 101, 6741-6748, 1996.

Newman, P. A., and E. R. Nash, Quantifying the wave driving of the stratosphere, *J. Geophys. Res.*, submitted, 2000.

Osterman, G. B., R. J. Salawitch, B. Sen, G. C. Toon, R. A. Stachnik, H. M. Pickett, J. J. Margitan, J. F. Blavier, and D. B. Peterson, Balloon-borne measurements of stratospheric radicals and their precursors: Implications for the production and loss of ozone, *Geophys. Res. Lett.*, 24, 1107-1110, 1997.

Randel, W. J., and F. Wu, Isolation of the ozone QBO in SAGE II data by singular value decomposition, *J. Atmos. Sci.*, 53, 2546-2559, 1996.

Randel, W. J., F. Wu, J. M. Russell III, A. Roche, and J. W. Waters, Seasonal cycles and QBO variations in stratospheric  $\text{CH}_4$  and  $\text{H}_2\text{O}$  observed in UARS HALOE data, *J. Atmos. Sci.*, 55, 163-185, 1998.

Randel, W. J., F. Wu, J. M. Russell III, and J. Waters, Space-time patterns of trends in stratospheric constituents derived from UARS measurements, *J. Geophys. Res.*, 104, 3711-3727, 1999.

Randel, W. J., F. Wu, and D. Gaffen, Interannual variability of the tropical tropopause derived from radiosonde data and NCEP reanalyses, *J. Geophys. Res.*, accepted, 2000.

Remsberg, E. E., J. M. Russell III, L. L. Gordley, J. C. Gille, and P. L. Bailey, Implications of stratospheric water vapor distributions as determined from the Nimbus 7 LIMS Experiment, *J. Atmos. Sci.*, 41, 2934-2945, 1984.

Remsberg, E. E., P. P. Bhatt, and J. M. Russell III, Estimates of the water vapor budget of the stratosphere from UARS HALOE data, *J. Geophys. Res.*, 101, 6749-6766, 1996.

Rosenfield, J. E., D. B. Considine, P. E. Meade, J. T. Bacmeister, C. H. Jackman, and M. R. Schoeberl, Stratospheric effects of Mount Pinatubo aerosol studied with a coupled two-dimensional model, *J. Geophys. Res.*, 102, 3649-3670, 1997.

Russell III, J. M., et al., The halogen occultation experiment, *J. Geophys. Res.*, 98, 10,777-10,797, 1993.

Russell III, J. M., M. Luo, R. J. Cicerone, and L. E. Deaver, Satellite confirmation of the dominance of chlorofluorocarbons in the global stratospheric chlorine budget, *Nature*, 379, 526-529, 1996a.

Scott, R. K., and P. H. Haynes, Internal interannual variability of the extratropical circulation: the low-latitude flywheel, *Quart. J. Roy. Meteor. Soc.*, 124, 2149-2173, 1998.

Siskind, D. E., L. Froidevaux, J. M. Russell III, and J. Lean, Implications of upper stratospheric trace constituent changes observed by HALOE for  $\text{O}_3$  and  $\text{ClO}$  from 1992 to 1995, *Geophys. Res. Lett.*, 25, 3513-3516, 1998.

Tie, X., G. P. Brasseur, B. Briegleb, and C. Granier, Two-dimensional simulation of Pinatubo aerosol and its effects on stratospheric ozone, *J. Geophys. Res.*, 99, 20,545-20,562, 1994.

World Meteorological Organization (WMO), Scientific Assessment of Ozone Depletion: 1998, *WMO Report 44*, Geneva, Switzerland, 1999

John Nash, UK Meteorological Office, Bracknell, Berkshire, UK

William J. Randel, Atmospheric Chemistry Division, National Center for Atmospheric Research, Boulder, CO 80303

J. M. Russell III, Center for Atmospheric Sciences, 23 Tyler Street, Hampton University, Hampton, VA 23668

Fei Wu, Atmospheric Chemistry Division, National Center for Atmospheric Research, Boulder, CO 80307

J. M. Zawodny, Atmospheric Chemistry Division, NASA Langley Research Center, Hampton, VA